Biophysical Chemistry 159 (2011) 162–171

Contents lists available at ScienceDirect

Biophysical Chemistry

journal homepage: http://www.elsevier.com/locate/biophyschem

Melting behavior and ligand binding of DNA intramolecular secondary structures

Souvik Maiti, Besik Kankia, Irine Khutsishvili, Luis A. Marky *

Department of Pharmaceutical Sciences, College of Pharmacy, University of Nebraska Medical Center, 986025 Nebraska Medical Center, Omaha, NE 68198-6025, United States

ARTICLE INFO

Article history:
Received 16 April 2011
Received in revised form 8 June 2011
Accepted 10 June 2011
Available online 21 June 2011

Keywords:
DNA stem-loop motifs
DSC and ITC calorimetries
DNA hydration
Netropsin binding
Density and ultrasound velocity techniques

ABSTRACT

We use a variety of biophysical techniques to determine thermodynamic profiles, including hydration, for the unfolding of DNA stem-loop motifs (hairpin, a three-way junction and a pseudoknot) and their interaction with netropsin and random cationic copolymers. The unfolding thermodynamic data show that their helix–coil transition takes place according to their melting domains or sequences of their stems. All hairpins adopted the B-like conformation and their loop(s) contribute with an immobilization of structural water. The thermodynamic data of netropsin binding to the $^{5'}$–AAATT–$^{3'}$/TTTAA site of each hairpin show affinities of ~10^{6-7} M^{-1}, 1:1 stoichiometries, exothermic enthalpies of −7 to −12 kcal mol^{-1} (−22 kcal mol^{-1} for the secondary site of the three-way junction), and water releases. Their interaction with random cationic copolymers yielded higher affinities of ~10^6 M^{-1} with the more hydrophobic hairpins. This information should improve our current picture of how sequence and loops control the stability and melting behavior of nucleic acid molecules.

1. Introduction

The function of nucleic acids is carried out *via* interactions with other molecules. In the readout of genetic information and in the control of gene regulation, the presence of proteins and other ligands is essential. Distinctive conformations are associated with the function of DNA. Sites of interaction of DNA with gene regulatory proteins have been found to exhibit characteristic conformational properties [1]. For instance, origins of replication in both procaryotes and eucaryotes appear to possess characteristic structural features. To understand how nucleic acids carry out their biological roles, it is essential to have a complete physical description of these interacting systems. In principle, the folding of nucleic acids is controlled by their base sequence in a precise and potentially predictable way. However, knowledge of the structure of a particular duplex alone cannot provide an understanding of the forces responsible for maintaining the distinct structures of nucleic acids. The overall physical properties of a nucleic acid molecule not only depend on its chemical architecture, but on contributions from base pairing, base stacking, ion and water binding.

The discovery of the human genome has led scientists to postulate the formation of additional unusual structures, including Holliday junctions, telomeres, i-motifs and triplexes. Furthermore, it has been demonstrated that palindromic sequences embedded in plasmids developed cruciform structures in response to a topological stress [2,3], which are cleaved by specific endonucleases [4,5]. These findings suggest that the presence of hairpin loops in DNA may play an important role in biological processes. Currently, there is considerable interest in both the structure and overall physical properties for the folding (and unfolding) of nucleic acid hairpin loops. Our current understanding of the structures and stability of both DNA and RNA has been enhanced by thermodynamic investigations of the helix–coil transitions of model oligonucleotide compounds, of known sequence [6–9]. Our laboratory is primarily interested in understanding the unfolding of single-stranded DNA oligomers that may adopt a variety of intramolecular secondary structures [10–12]. Their monomolecular unfolding takes place with a lower entropy penalty yielding transition temperatures higher than their bimolecular counterparts, allowing investigations of the physical properties of their 100% helical conformations over a wider temperature range [13].

Netropsin is a natural oligopeptide that binds in the minor groove of B-DNA with high affinity and specificity for stretches of dA·dT base pairs. The netropsin–DNA complexes are stabilized by a combination of hydrogen bonding, van der Waals and electrostatic interactions, and the extent of these interactions depends on how well netropsin penetrates the minor groove [14,15].

Experimental and theoretical investigations have indicated that water plays a fundamental role in the stability and overall secondary structure of nucleic acids. Nucleic acid helical structures are heavily hydrated [16–20]. Their overall hydration in solution depends on their conformation, nucleotide composition and sequence [21–28]. However, the detailed nature of this phenomenon remains unclear, and this is due to the simultaneous presence of two distinctive types of hydrating water around a nucleic acid molecule: hydrophobic or structural (around polar and non-polar groups) and electrostricted

* Corresponding author. Tel.: +1 402 559 4628; fax: +1 402 5599543.
E-mail address: lmarky@unmc.edu (L.A. Marky).

0301-4622/$ – see front matter
doi:10.1016/j.bpc.2011.06.006

(around charged groups) [29,30]. These two types of water are difficult to detect and differentiate, complicating the measurement and analysis of their physical properties. Furthermore, nucleic acid hydration is closely associated with its number and type of counterions because these ions are also hydrated [31–33].

Since 1995, all members of our laboratory have attended the annual Gibbs meeting. This meeting has served as a forum for discussion of our experimental results, and our graduate students need to have an oral presentation as part of their PhD requirements. Everyone has enjoyed these meetings because of the common thermodynamic language of all participants. For this special issue commemorating the 25th anniversary of the Gibbs meetings on Biological Thermodynamics, our contribution includes all four aspects of our investigations with nucleic acids. These include the folding/unfolding energetics of nucleic acids as a function of sequence, conformation and solution conditions; their interaction with ions and ligands; hydration properties of nucleic acids and their hydration effects upon ligand binding; and current investigations on the interaction of DNA oligonucleotides with polycations for the purpose of their cellular delivery to control the expression of genes.

In this work, we present a thermodynamic description, including hydration, of the unfolding of three DNA oligonucleotides forming intramolecular stem-loop motifs, and their interaction with both netropsin and random cationic copolymers. Specifically, we used a combination of UV and circular dichroism spectroscopies, calorimetric techniques, density and ultrasound techniques to investigate both the unfolding thermodynamics, including hydration effects, of a hairpin loop, three-way junction, and *Pseudoknot*. We also investigated the binding thermodynamics, and associated hydration effects, for the interaction of netropsin with the $d(A_3T_2)/d(T_3A_2)$ site of each hairpin. The hydrophobic contribution of their loops was probed by looking at their interaction with random cationic copolymers as a function of their percentage of polyethylene glycol.

2. Materials and methods

2.1. Materials

We used the following oligonucleotides (and their designations) with 5′ to 3′ sequences: $GA_3T_2C_5A_2T_3C$ (*Hairpin*), $GA_3T_2GCGCT_5$-$GCGCGTGCT_5GCACA_2T_3C$ (*Hammer*), and $CGCGCGT_4GA_3T_2CGCGCGT_4$-$A_2T_3C$ (*Pseudoknot*), their putative secondary structures are shown in Fig. 1. All oligonucleotides were synthesized in the Eppley Institute Molecular Biology Core Facility at UNMC, reverse-phase HPLC purified, desalted on a G-10 Sephadex column, and lyophilized to dryness. The concentration of each oligomer solution was determined from absorbance measurements at 260 nm and 80 °C using the following molar absorptivities in $mM^{-1}\,cm^{-1}$ of strands: 164 (*Hairpin*), 344 (*Hammer*), and 309 (*Pseudoknot*). These values were calculated by using procedures reported earlier [34,35]. Netropsin, from Sigma, was used without further purification. Random cationic copolymers were synthesized from methoxy poly(ethylene glycol) monomethacrylate (MePEGMA) and (3-(mathacryloylamino)-propyl)trimethylammonium chloride (MAPTAC) with different mole ratios (38:62, 51:49, and 68:32). A full description of their synthesis has been reported elsewhere [36]. All other chemicals were of reagent grade. The buffer solutions consisted of 10 mM sodium phosphate, 0.1 M NaCl at pH 7 or 10 mM Hepes, 100 mM NaCl, at pH 7.5.

2.2. Temperature-dependent UV spectroscopy

UV melting curves, as a function of strand- and salt concentration, were measured at 260 nm with a thermoelectrically controlled Aviv 14 DS UV/Vis spectrophotometer (Lakewood, NJ). The absorbance was scanned with a temperature ramp of ~0.4 °C/min. The analysis of the shape of the melting curves yielded transition temperatures, T_Ms, and van't Hoff enthalpies, ΔH_{vH}s [37]. We investigated the molecularity of each transition from the T_M-dependence on strand concentration, constant T_M indicates an intramolecular transition.

2.3. Circular dichroism spectroscopy (CD)

We use a thermoelectrically controlled Aviv circular dichroism spectrometer Model 202SF (Lakewood, NJ) to measure the CD spectrum of each oligonucleotide. Typically, we prepared a hairpin buffered solution with an absorbance of 1 (~4 μM in strands), and the CD spectrum was measured from 320 to 200 nm every 1 nm, using a strained free quartz cuvette with a pathlength of 1 cm, at temperatures such that the particular hairpin is 100% helical. The reported spectra correspond to an average of at least two scans.

To obtain the stoichiometry of each netropsin-hairpin, a hairpin solution was titrated with a netropsin solution, and the induced ellipticity of the bound netropsin was followed at 310 nm. The plots of

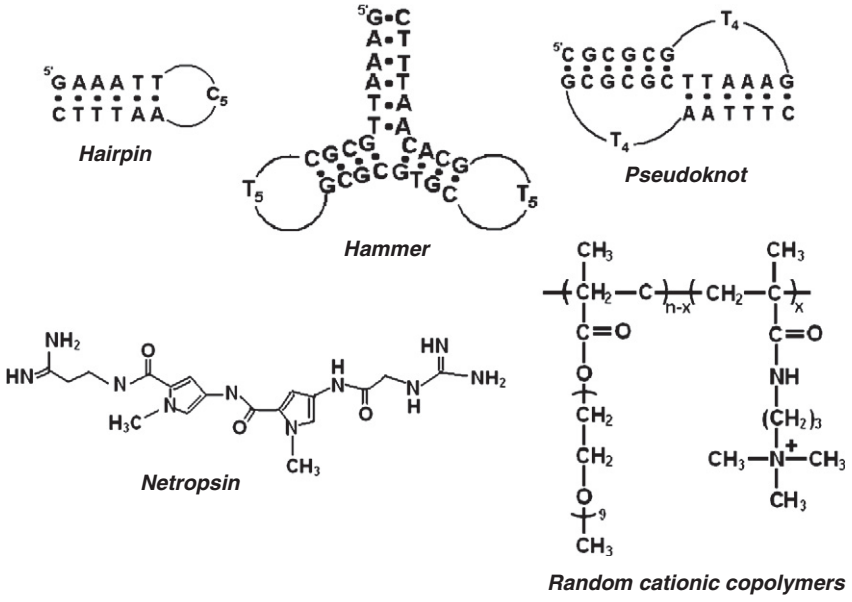

Fig. 1. Sequences, designation and cartoon of intramolecular DNA stem-loop motifs.

ellipticity vs. [netropsin]/[hairpin] molar ratio yielded the stoichiometry of each complex from the breaks of the two intersecting lines [15,38,39].

2.4. Differential scanning calorimetry (DSC)

Heat capacity functions of the helix–coil transition for each hairpin were measured with a Microcal VP-DSC (Northampton, MA) instrument. Two cells, the sample cell containing 0.5 mL of a DNA solution (~0.15 mM in total strands) and the reference cell filled with buffer solution, were heated from 0 °C to 90 °C at a heating rate of 0.75 °C/min. A buffer vs. buffer scan was also done under similar conditions and subtracted from the subsequent experimental runs; the resulting curve was normalized for the number of moles. Analysis of these thermographs yielded T_Ms and standard thermodynamic unfolding profiles: ΔH_{cal}, ΔS_{cal} and $\Delta G^{\circ}_{(T)}$[37]. These parameters are measured with the following relationships: $\Delta H_{cal} = \int \Delta C_p^a dT$ and $\Delta S_{cal} = \int (\Delta C_p^a/T) dT$, where ΔC_p^a represents the heat capacity during the unfolding process [37]. The free energy, $\Delta G^{\circ}_{(T)}$, is obtained at any temperature with the Gibbs relationship: $\Delta G^{\circ}_{(T)} = \Delta H_{cal} - T\Delta S_{cal}$. Alternatively, $\Delta G^{\circ}_{(T)}$ can be obtained using the following equation for intramolecular transitions: $\Delta G^{\circ}_{(T)} = \Delta H_{cal}\,(1 - T/T_M)$. For multiphasic unfolding curves, the heat associated with each transition is obtained using a non two-state deconvolution procedure in the Origin software, provided with the VP-DSC instrument. To determine netropsin binding affinities, K_bs, additional DSC curves were obtained for solutions of netropsin–hairpin complex at 1:1 [netropsin]/[hairpin] molar ratios. The K_bs were obtained from the increase in the T_Ms of each saturated complex relative to the free hairpin [15].

2.5. Differential thermodynamic binding of counterions

The Helix → Coil transition of a hairpin is accompanied by a release of counterions, Δn_{ion}, due to the higher charge density parameter of the helical state [40,41]. This Δn_{ion} term is measured with the assumption that counterions bind similarly to the helical and coil states [40]. We used the equation [42]:

$$\Delta n_{Na^+} = 0.483\left[\Delta H_{cal} / RT_M^2\right]\left(\partial T_M / \partial \log\left[Na^+\right]\right). \quad (1)$$

The 0.483 factor results from the conversion of natural to decimal logarithms and ionic activities into concentrations, the $[\Delta H_{cal}/RT_M^2]$ term is determined in DSC experiments, R is the gas constant; and the term in parenthesis is determined from the T_M-dependence on salt.

2.6. Isothermal titration microcalorimetry (ITC)

The heats of netropsin binding to each hairpin were measured directly by ITC using the iTC_{200} calorimeter from Microcal, Inc. A detailed description of this instrument has been presented elsewhere [43,44]. In a typical titration, 24–48 injections of 0.5–2.5 μL each were performed in a single and continuous titration. A 40 μL syringe filled with netropsin solution (0.10–0.74 mM) was used to titrate 300 μL of hairpin solution (5.3–77 μM) (200 μL is the effective reacting volume of this cell). Complete mixing is achieved by stirring of the syringe paddle at 1000 rpm. The reference cell of the calorimeter was filled with water. The area under the resulting peak following each injection is proportional to the interaction heat, Q. After Q is corrected for the dilution heat of the titrant and normalized by the concentration of bound ligand, it yields the binding enthalpy, ΔH_b. The precision on the injection heats is ~0.1 μcal. Analysis of the calorimetric binding isotherm, yields ΔH_bs, binding affinities (K_b) and complex stoichiometries (n). The resulting calorimetric binding isotherm corresponds to the dependence of (Total Heat)/(mole of netropsin injected) on the [Netropsin]/[hairpin] ratio. The binding isotherm of *Hairpin* was fitted to a model that incorporates a coupling of netropsin binding with hairpin-duplex conformational changes, as described earlier [45], while the other binding isotherms were fitted with the Origin software (version 7), supplied by Microcal Inc., using one (*Pseudoknot*) or two sets (*Hammer*) of three parameters, K_b, ΔH_b and stoichiometries (n).

2.7. Density and ultrasonic velocity measurements

The density of each hairpin solution was measured with a DMA-602 densimeter (Anton Paar, Graz, Austria) with two 200 μL cells. The apparent molar volume, ΦV, is calculated using the equation [31]: $\Phi V = M/\rho - (\rho - \rho_o)/(\rho_o C)$, where ρ_o and ρ are the density of the solvent and solution, respectively, M is the molecular weight of the hairpin, and C its concentration. Ultrasonic velocity measurements were obtained in the frequency range of 7–8 MHz with a home built instrument, based on the resonator method [46], using two cells differentially. The molar increment of ultrasonic velocity, A, is defined by the equation: $A = (U - U_o)/(U_o C)$, where U and U_o are the ultrasonic velocities of the solution and solvent, respectively, and C is the solute concentration. The experimental error in the measurement of $(U - U_0)/(U_0)$ is 2×10^{-5}%. The molar adiabatic compressibility, ΦK_S, is obtained from equation [47]: $\Phi K_S = 2\beta_o(\Phi V - A - M/2\rho_o)$, where β_o is the adiabatic compressibility coefficient of the solvent.

The molecular interpretation for the absolute ΦV and ΦK_S parameters is provided by the relationships [48]: $\Phi V = V_m + \Delta V_h$ and $\Phi K_S = K_m + \Delta K_h$. The V_m term is the intrinsic molar volume of the solute, and K_m is the intrinsic molar compressibility of this volume that is inaccessible to the surrounding solvent. The ΔV_h term represents the hydration contribution of the change in the volume of water surrounding the solute. The ΔK_h term is the hydration contribution of the change in the compressibility of water around a solute and the compressibility of the void volumes, if any, between the solute and that of the surrounding water. For oligonucleotides, the contribution of K_m is small relative to ΔK_h. Therefore, the value of ΦK_S reflects the sole hydration contribution, i.e., $\Phi K_S = \Delta K_h$.

The molar volume change, ΔV, accompanying the interaction of netropsin with each hairpin is calculated from the relationship: $\Delta V = (m_1\rho_1 + m_2\rho_2 - m_{12}\rho_{12})/(m_1\rho_1 C_1)$, where m and ρ correspond to the mass and density for each of the reagents, 1 (netropsin) or 2 (hairpin) and product complex (12). One of the reagents is considered limiting. The change in the molar increment of ultrasound velocity, ΔA, accompanying the interaction of netropsin with each hairpin is given by the relationship: $\Delta A = (m_{12}U_{12} - m_1U_1 - m_2U_2)/(m_1U_0C_1)$; where m_1, m_2 and m_{12} are the masses of each reactant and the mass of the product complex, respectively; U_1, U_2 and U_{12} are the corresponding ultrasound velocities of the solutions of each reactant and product, respectively, and C_1 is the molar concentration of reagent 1 (netropsin). All ΔA values were calculated in terms of the netropsin concentration. In these acoustically monitored titrations, each hairpin is titrated with netropsin. 2−5 μL aliquots of netropsin were added stepwise, using calibrated 10 μL Hamilton syringes, to 695 μL hairpin solution in the sample cell. Mixing was performed with a built-in magnetic stirrer. The reference cell was filled with water. The resulting ΔA values were corrected for dilution effects, by subtracting the ΔA values of a similar titration of the buffer. The change in the molar adiabatic compressibility, ΔK_S, is determined with the relationship [47]: $\Delta K_S = 2\beta_0(\Delta V - \Delta A)$. In the absence of significant conformational changes, both V_m and K_m values remain constant, indicating that the ΔV and ΔK_S values reflect their hydration changes, i.e., $\Delta V = \Delta\Delta V_h$ and $\Delta K_S = \Delta\Delta K_h$.

2.8. Ethidium displacement assay

The displacement of bound ethidium from DNA is followed with the increase in copolymer concentration to determine copolymer binding affinities, K_{pol}, with each hairpin. An Aviv ATF 105

spectrofluorometer is used to measure the emission spectrum of the DNA bound ethidium as a function of the copolymer concentration, using an excitation wavelength of 480 nm. The fluorescence intensity of the DNA solutions with ethidium (at 600 nm) in the absence of copolymer was set to 0% ethidium released, and the fluorescence of free ethidium was set to 100% ethidium released. The percentage of ethidium released was plotted vs. the copolymer concentration added into the solution and the copolymer concentration excluding 50% ethidium, C_{50}, is obtained from this plot. This C_{50} term is proportional to K_{pol} according to the equation [49]: $K_{EB} \times C_{EB} = K_{cop} \times C_{50}$, where K_{EB} is the binding affinity of ethidium for each hairpin, determined from independent fluorescence experiments by titrating an ethidium solution with stepwise additions of a concentrated hairpin solution under similar solution conditions, and C_{EB} is the initial molar concentration of ethidium bound to DNA.

3. Results and discussion

3.1. UV melting curves

The helix–coil transition of each hairpin (Fig. 1) was characterized initially by UV melting curves (Fig. 2a). All three UV melting curves show the characteristic melting behavior of the cooperative unfolding of base pairs and base-pair stacks of oligonucleotides; however, *Hairpin* shows one transition, *Hammer* has 2–3 transitions, while *Pseudoknot* shows two distinctive transitions. The T_Ms for the transitions of each oligonucleotide remain constant, despite the ~100 fold increase in strand concentration (Fig. 2b) consistent with its intramolecular unfolding. The T_Ms of the transitions of each hairpin molecule, Table 1, corresponds roughly to the percentage of GC base pairs in their helical stems. Furthermore, the T_M of the first transition of each hairpin corresponds to the unfolding of their GA_3T_2/CT_3A_2 stem. We obtained T_Ms of 35.8 °C (*Hairpin*), 31.3 °C (*Hammer*) and 45 °C (*Pseudoknot*). The analysis of the shape of this transition for each hairpin, using standard procedures [37], yielded the following ΔH_{vH}s: −37 kcal mol^{-1} (*Hairpin*); −26, kcal mol^{-1} (*Hammer*), and −12 kcal mol^{-1} (*Pseudoknot*). These values clearly indicate the effects of the adjacent secondary structure of this stem, C_5 end loop, three-way crossover junction and T_4 loop, respectively, in reducing the enthalpy contributions. The CD spectrum of each hairpin (Fig. 2c) indicates the hairpins adopting the B-like conformation, as seen by the similar magnitudes between the longer wavelength positive band and the negative band centered at 250 nm.

3.2. DSC unfolding of hairpins

Typical DSC profiles are shown in Fig. 3a. These curves clearly show that the DNA unfolding is monophasic (*Hairpin*), triphasic (*Hammer*), and biphasic (*Pseudoknot*), consistent with the observations of the UV melting curves. Thermodynamic profiles for all transitions observed in the folding of each oligonucleotide are listed in Table 1. The thermodynamic parameters of each transition show that the favorable free energy contribution results from the characteristic compensation of a favorable enthalpy contribution with an unfavorable entropy contribution. Favorable heat contributions involve the formation of base pairs and base-pair stacks, whereas unfavorable entropy contributions involve the ordering of the strands, ion and water binding. The enthalpy contributions of each transition are in good agreement with the expected enthalpy values from nearest-neighbor calculations [6,8]. For instance, in 0.1 M NaCl, we obtained enthalpy contributions of 36.7 kcal mol^{-1} (*Hairpin*) and 36.4 kcal/mol^{-1} for the first transition of *Hammer*), which are in excellent agreement with the value of 39.9 kcal mol^{-1} estimated from nearest-neighbor parameters in 1 M NaCl [6,8]; however, the enthalpy of the first transition of *Pseudoknot* is much lower, by 9.3 kcal mol^{-1}, in spite of having similar helical sequence. The overall effects are explained in terms of the actual contribution of the adjacent secondary structure, in the case of *Hairpin* and *Hammer*, the loop and crossover junction

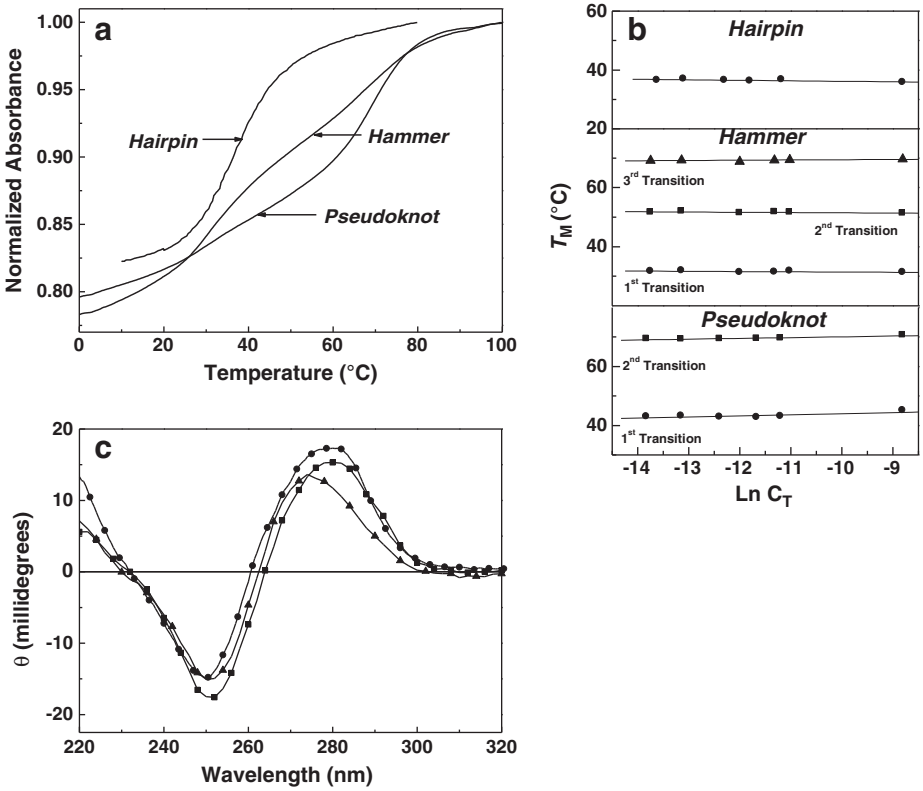

Fig. 2. a) Typical UV-melting curves of hairpin molecules. b) T_M-dependence on strand concentration. c) CD spectra of hairpin molecules at 10 °C: *Hairpin* (circles), *Hammer* (squares), *Pseudoknot* (triangles). All experiments in 10 mM sodium phosphate buffer, 0.1 M NaCl at pH 7.

Table 1
Thermodynamic profiles for the folding of hairpins.

	T_M (°C)	ΔH_{cal} (kcal/mol)	$T\Delta S_{cal}$ (kcal/mol)	$\Delta G^o_{(15)}$ (kcal/mol)	Δn_{Na+} (mol Na^+/mol)	ΦV (cm^3/mol)	$\Phi K_S \times 10^4$ (cm^3/mol bar)
Hairpin							
	35.8	−37.5	−2.5	−34.8	0.06	138.8	−111.6
Hammer							
1st	31.3	−35.1	−1.9	−34.5	0.03	120.7	−132.6
2nd	51.3	−23.6	−2.6	−21.0	nd		
3rd	69.6	−36.2	−5.8	−30.4	0.13		
Pseudoknot							
1st	45.0	−27.2	−2.3	−24.9	0.03	129.1	−118.7
2nd	70.6	−48.6	−7.8	−40.8	0.10		

All UV and DSC experiments were measured in 10 mM sodium phosphate buffer, 0.1 M NaCl at pH 7, whereas the hydration parameters were determined in 10 mM Hepes, 0.1 M NaCl, pH 7.5 at 15 °C, and are calculated per mole of nucleotide. Experimental uncertainties are as follows: T_M (±0.5 °C), ΔH_{cal} (±3%), $T\Delta S_{cal}$ (±3%), $\Delta G^o_{(15)}$ (±5%), Δn_{Na+} (±5%), ΦV (±8), and ΦK_S ($\pm 13\times10^{-4}$).

has no effect, while the T_4 loop of *Pseudoknot* lies on the ceiling of the sugar-phosphate backbone that removes water, reducing its enthalpy contribution.

In terms of the overall free energy contribution of folding each hairpin at 15 °C, we obtained ΔG^os contributions of −2.5 kcal mol^{-1} (*Hairpin*), −10.3 kcal mol^{-1} (*Hammer*) and −10.1 kcal mol^{-1} (*Pseudoknot*). This indicates that each molecule folds with their particular secondary structure at 15 °C, and the overall thermodynamic profiles for each transition of these hairpins are consistent with the sequences of their melting domains. The entropy contributions, in energy terms ($T\Delta S_{cal}$), for the formation of each melting domain are shown in the fourth column of Table 1. The magnitude of these unfavorable entropy terms follow the same order as those of the enthalpies, and correspond to contributions of the ordering of the oligonucleotide, uptake of counterions, and the immobilization of water molecules by the helical states of each hairpin. These two later contributions are discussed in the following sections.

We measured the uptake of counterions, using Eq. (1), from the T_M-dependence on salt concentration (Fig. 3b), and the $\Delta H_{cal}/RT_M^2$ terms obtained in the DSC curves. For each transition, the increase in salt concentration shifts the melting curves to higher temperatures (data not shown), due to the shift of the hairpin–coil equilibrium towards the conformation with higher charge density parameter. The T_M-dependence on salt concentration for each hairpin is shown in Fig. 3b (with the exception of the 2nd transition of *Hammer* that was difficult to determine), linear dependences are obtained with slope values ranging 2.3 to 2.9 °C. The resulting Δn_{Na}^+ values are shown in the sixth column of Table 1. The magnitude of these values indicates the strength of ion binding by the helical state of each molecule. Relative to the value of 0.17 mol Na^+/mol phosphate for longer duplex DNA molecules, these values are low but consistent with the formation of five base pairs in the hairpin stems [50]. The higher uptake of counterions by helical stems with exclusively G·C base pairs is consistent with the published observation that the major groove of G·C base pairs is preferred ion binding sites [51].

3.3. Hydration parameters of hairpins

The ultrasound velocity and density of the hairpin solutions have been measured to characterize the overall hydration of each hairpin. The resulting ΦV and ΦK_S values for each hairpin are shown in the last two columns of Table 1, all ΦV values are positive, while all ΦK_S are

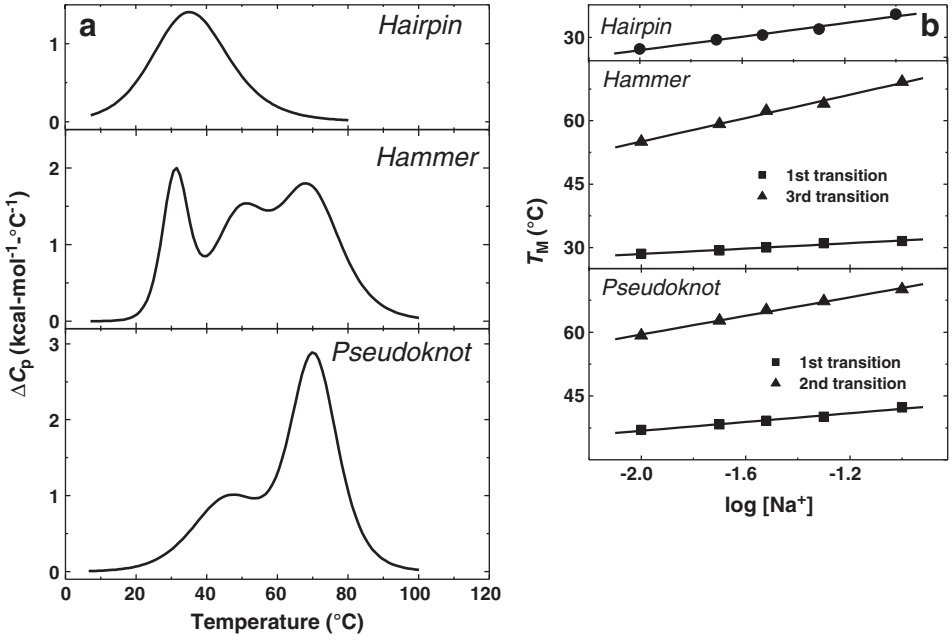

Fig. 3. a) Heat capacity profiles for the hairpin molecules in 10 mM sodium phosphate buffer, 0.1 M NaCl at pH 7. b) T_M-dependence on salt concentration for all transitions of each hairpin (the second transition of *Hammer* was not determined).

negative, which is typical of nucleic acid molecules. The ranges of the ΦV values, 120.7 to 138.8 cm^3/mol, and ΦK_S values, -111.6×10^{-4} to -132.6×10^{-4} cm^3/mol bar are in very good agreement with earlier measurements of oligonucleotides [52]. The values of ΦV are positive because the magnitudes of the intrinsic volumes (V_ms>0) exceed the corresponding negative hydration terms (ΔV_hs<0). The negative ΦK_S values are determined by the fact that molecules with high packing coefficients are characterized by negligible intrinsic contributions in comparison to the negative hydration term; therefore, the ΦK_S values can be interpreted in terms of hydration. In general, a decrease in ΦK_S corresponds to an increase in the extent of hydration. For these hairpins, the following order of ΦK_S values is observed: *Hairpin*> *Pseudoknot*>*Hammer*, corresponding to increasing hydration from *Hairpin* to *Hammer* molecules. A rigorous comparison among these hairpin molecules is not possible, due to their differences in nucleotide sequence and structure. However, the plot of ΦV vs. ΦK_S (Fig. 4) yielded a positive slope, $k=0.8\times10^4$ bar, which indicates the type of water in the hydration shells of these hairpins [53]. For instance, k values of $0.3–0.4\times10^4$ bar are characteristic of dissolved charged molecules [54] and of their interactions between themselves [55,56], dissolved DNA duplexes have ks of $\sim0.6\times10^4$ bar [32,57], whereas the k values of the nucleic acid bases are $\sim0.8\times10^4$ bar [58]. The formation of a nucleic acid duplex, which is accompanied by an uptake of water molecules, has a $k=0.8\times10^4$ bar [52]. Therefore, the resulting slope of 0.8×10^4 bar of Fig. 4 indicates that the hydration shell of these hairpins primarily consists of structural water.

3.4. Interaction of netropsin to the A_3T_2 site of each hairpin

An $^{5'}$–AAATT–$^{3'}$/TTTAA (A_3T_2) sequence was placed at the end stem of each hairpin (Fig. 1) to interact with netropsin. The rationale behind this design is two-fold: a) binding of netropsin to this stem should confirm the formation of each hairpin, and b) to test the effects of the adjacent secondary motif on netropsin binding. For example, the A_3T_2 binding site in the stem of *Hairpin* is adjacent to a loop, in *Hammer* it is next to a three-stem junction, whereas in *Pseudoknot* this site is partially covered by a loop of four thymines.

3.4.1. Stoichiometry of netropsin–hairpin complexes

The CD spectra of the hairpins are shown in Fig. 5 in the presence and absence of netropsin. The addition of netropsin to each hairpin results in significant ellipticity (θ°) changes, except at the well defined isoelliptic points, which indicates the presence of an equilibrium of a free and bound netropsin (Fig. 5 a,b). The bound netropsin shows an induced Cotton effect, best indicated by an extra band at ~310 nm. We used this wavelength to monitor netropsin binding, because the DNA contributions are negligible. The resulting titration curves are shown in Fig. 5b. The major breaks of the lines correspond to 1:1 stoichiometries for each hairpin; consistent with our earlier investigations that one netropsin molecule is accommodated in the minor groove of the A_3T_2 site of a duplex [15]. However, an additional and less evident break is seen in the *Hammer* titration at a [netropsin]/[hairpin] ratio of 2. Similar stoichiometries were obtained with *Hammer* and *Pseudoknot* in the ITC titrations, whereas ultrasonic velocity titrations yielded 1:1 stiochiometries with all three hairpins, as discussed in later sections.

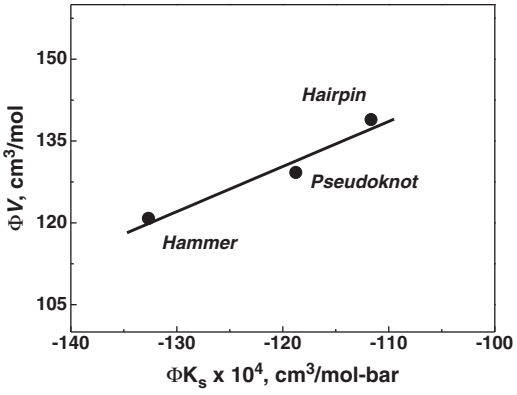

Fig. 4. Plot of the absolute values of ΦV and ΦK_S. The slope of the line is equal to 0.8 bar, this empirically indicates that the hydration of each hairpin is dominated by structural water.

3.4.2. Netropsin binding results in exothermic heats

The heat of netropsin interacting with each hairpin was determined directly by ITC from averaging the heats of multiple (5 to 12) injections under unsaturating conditions, see Fig. S1 for solution conditions. After correcting for the netropsin dilution heat, we obtained ΔH_bs of -8.9 kcal mol^{-1} (*Hairpin*), -7.6 kcal mol^{-1} (*Hammer*) and -12.2 kcal mol^{-1} (*Pseudoknot*), which are in agreement with the ΔH_b of -7.5 kcal mol^{-1} obtained earlier with an identical site in a duplex [15]. The higher ΔH_b with *Pseudoknot* is explained in terms of additional van der Waals contributions involving its thymine loop. Calorimetric titrations for all netropsin–hairpin complexes are shown in Fig. 6. The curves show initial ΔH_bs of -7 kcal mol^{-1} (*Hairpin* and *Hammer*) and -10 kcal mol^{-1} (*Pseudoknot*), which get more exothermic for *Hairpin* (-13 kcal mol^{-1}) and *Hammer* (-18 kcal mol^{-1}) upon reaching saturation; further addition of netropsin yielded ΔH_bs close to zero. The stoichiometries in these curves are roughly: 1:1 (*Hairpin* and *Pseudoknot*) and 2:1 (*Hammer*). The initial heats are consistent with earlier measurements for the interaction of netropsin with DNA polymers and oligonucleotides [15,59,60]. However, the observed increase in exothermicities of *Hairpin* and *Hammer*is unusual and corresponds to ligand binding induced events. In the case of *Hairpin*, netropsin induces dimerization of hairpin, forming duplexes with one and two netropsin molecules, yielding an overall stoichiometry of 1:1, as reported earlier in the interaction of this ligand with hairpin loops [45]. In the case of *Hammer*, netropsin binding is optimizing base-pair stacking on the adjacent three-stem junction, forming a secondary site.

We have tried different models to fit the experimental binding isotherms, including the global fitting model for the netropsin–*Hairpin* system that incorporates the equilibria of four reactions involving netropsin with the hairpin and duplex states of *Hairpin* [45]. The results of these fitting procedures are shown in Table 2, while the complete set of binding parameters for the netropsin–*Hairpin* system is shown in Table S2. The resulting curves of the fits are included in Fig. 6. These solid lines fit the experimental binding isotherms very well and the best fitting estimates are obtained with one set of parameters (*Pseudoknot*) and two sets of parameters (*Hammer*); each set has roughly 1:1 stoichiometries. The single binding of netropsin to the A_3T_2 site of each hairpin is accompanied by exothermic enthalpies (in kcal mol^{-1}) of -7.0 (*Hairpin*), -7.6 (*Hammer*), and -12.2 (*Pseudoknot*); and, K_bs ranging from 1.2×10^5 (*Pseudoknot*) to 5.2×10^7 (*Hammer*), see Table 2. The K_b values of *Hairpin* and *Hammer* are in excellent agreement with the average K_b value of 4.5×10^7 obtained previously [15]. However, binding to the A_3T_2 site of *Pseudoknot* is ~300 fold lower, which may be due to the presence of the nearby thymine loop that is interfering.

The global fitting of the netropsin–*Hairpin* binding isotherm clearly shows that netropsin induces the dimerization of *Hairpin*, the *K*s and enthalpy parameters for the four reactions included in this fitting procedure are shown in Table S2. The fitting of the netropsin–*Hammer* binding isotherm yielded a secondary site, characterized with a lower K_b (2×10^6 M^{-1}) and higher ΔH_b (-21.5 kcal mol^{-1}). This site may be the adjacent three-way junction or the $^{5'}$–GCAC/$^{5'}$–GTGC stem; the high exothermic term favors the site at the junction in a way that binding of a second netropsin molecule may induce a more compact *Hammer*, by

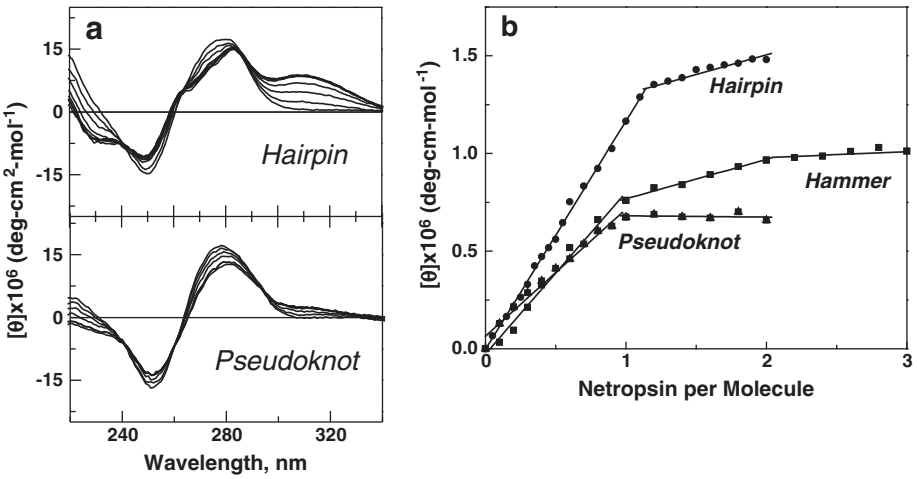

Fig. 5. a) CD spectra of *Hairpin* and *Pseudoknot* in the presence of different netropsin concentrations at 10 °C. b) Typical titration curves of each hairpin with netropsin: *Hairpin* (circles), *Hammer* (squares) and *Pseudoknot* (triangles).

forming 1 to 2 additional base-pair stacks at the junction site. In this case, netropsin binds to a site with a high content of dG·C base pairs, yielding a small signal in its CD titration (Fig. 5b). The last column of Table 2 corresponds to K_bs obtained from DSC (Fig. S2) and UV melting curves (data not shown) of the 1:1 netropsin–hairpin complexes, 2:1 netropsin–*Hammer* complex, and free ligand hairpins. These K_b values are determined from the increased in thermal stability (ΔT_M) of the saturated complexes relative to the free hairpins [15]. All of the experimentally determined parameters used in this determination are shown in Table S1. The resulting K_bs (the last column of Table 2) are in excellent agreement with the ones obtained in the fits of the ITC binding isotherms.

3.4.3. Volume and compressibility effects of netropsin binding

Ultrasonic velocity titrations of netropsin with each hairpin (Fig. S3) show two intersecting lines with breaks that correspond to 1:1 stoichiometries for each hairpin, which are consistent with the CD and ITC results. The ΔV and the derived ΔK_S for the formation of the 1:1 netropsin–hairpin complex, using netropsin as the limiting reagent, are listed in the last two columns of Table 3. The positive values of both ΔV and ΔK_S parameters indicate that the effects are determined mainly by a hydration process, and not by the intrinsic volume and intrinsic compressibility changes of the hairpins. These positive values show that complex formation is accompanied by a release of water molecules. Similar water releases (ΔV of ~38 cm^3/mol) are obtained for *Hairpin* and *Hammer*, while the release of water is smaller for the *Pseudoknot* (30.8 cm^3/mol). This is in good agreement with earlier ΔV measurements of netropsin binding to poly(dA)·poly(dT) and poly[d(AT)]·poly[d(AT)], that yielded ΔVs of 40–68 cm^3/mol and −1 cm^3/mol, respectively [59,61]. The type of hydrating water is characterized empirically by the $\Delta V/\Delta K_S$ ratio. We obtained $\Delta V/\Delta K_S$ ratios of 0.4×10^4 bar (*Hairpin* and *Hammer*), indicative of a release of electrostricted water, and 0.7×10^4 bar (*Pseudoknot*), which indicates a release of structural water. The number of water molecules, N, involved in the binding event can be estimated from the ΔV values (Table 3) and the equation: $N = \Delta V/(V_h - V_w)$, where V_h is the molar volume of water released by the hydration shells, and V_w is the molar volume of bulk water (equal to 18 cm^3/mol). The change of the molar volume of electrostricted water has been determined to be equal to 2.5 cm^3/mol [31,60], and for structural water is equal to 4.5 cm^3/mol

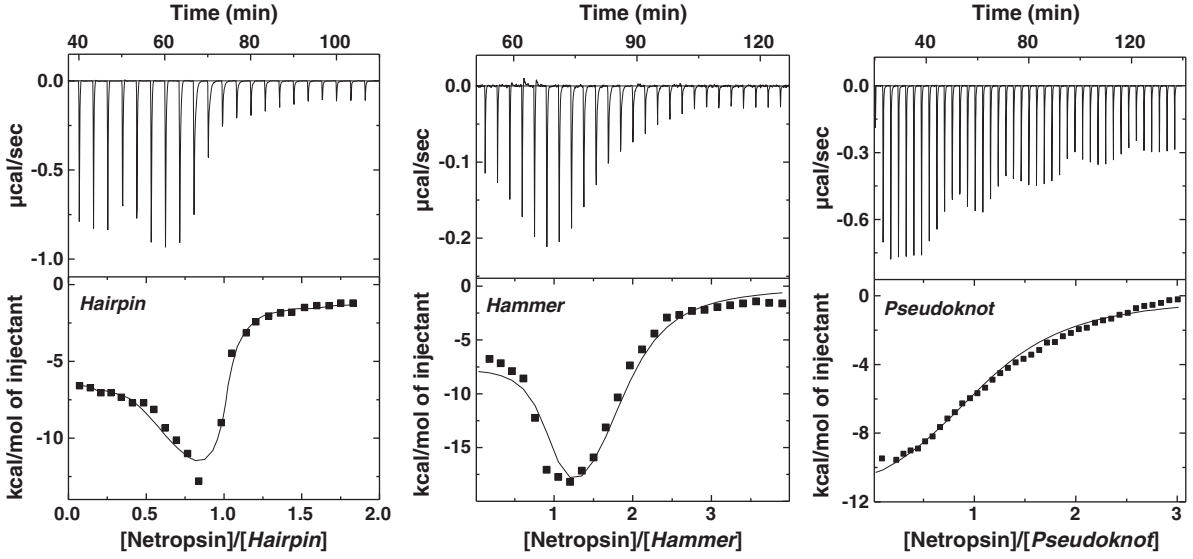

Fig. 6. Isothermal calorimetric titration curves for netropsin–hairpin complexes in 10 mM sodium phosphate buffer, 0.1 M NaCl, at pH 7 and 10 °C. The solution concentrations used of hairpin and netropsin are as follows: *Hairpin* (77 μM, 740 μM), *Hammer* (5.3 μM, 100 μM) and *Pseudoknot* (45 μM, 636 μM), respectively.

Table 2
Netropsin binding profiles from ITC and DSC and UV melts.

Site	ITC fitting			DSC		
	n	ΔH_b (kcal/mol)	$K_b \times 10^{-7}$ (M^{-1})	ΔT_M (°C)	ΔH_{cal} (kcal/mol)	$K_b \times 10^{-7}$ (M^{-1})
Hairpin						
A_3T_2	nd	−7.0	2.6	27.8	−37.5	2.1
Hammer						
A_3T_2	0.9	−7.4	5.2	29.2	−35.1	1.2
Secondary	0.9	−21.5	0.2	1.2	−29.9	0.2
Pseudoknot						
A_3T_2	1.1	−12.5	0.01	9.7	−27.2	0.1

All experiments were measured in 10 mM sodium phosphate buffer, 0.1 M NaCl at pH 7 and 10 °C. Experimental uncertainties are as follows: n (±10%), ΔH_b (±5%), K_b (±30%), and ΔT_M (±0.7 °C).

[62]. This procedure yielded the following *N* values, per mole of netropsin: release of 15 electrostricted water molecules (*Hairpin* and *Hammer*) and a release of 7 structural water molecules (*Hammer*).

3.4.4. Thermodynamic profiles for the interaction of netropsin to each hairpin

Complete thermodynamic profiles for the interaction of netropsin to each hairpin at 10 °C are summarized in Table 3. The listed K_bs correspond to the average of the experimentally determined K_b from two different methods, the free energies are calculated by using the standard thermodynamic relationship, $\Delta G^\circ_b = -RT \ln K_b$, the ΔH_bs are obtained from the fits of the ITC titrations, while the entropy contributions from the Gibbs equation, $\Delta G_b^\circ = \Delta H_b - T\Delta S_b$. Similar favorable free energy terms (−9.5 kcal/mol^{-1}) are obtained for the binding of netropsin to the A_3T_2 site of *Hairpin* and *Hammer*, resulting from favorable enthalpy and entropy contributions; while for *Pseudoknot*, a 2.1 kcal less favorable ΔG_b° term is obtained that is enthalpy driven. Favorable enthalpy contributions involve exothermic contributions from hydrogen bonding and van der Waals contacts with the walls of the minor groove, while favorable entropy contributions include the release of water molecules and the putative release of counterions, due to the cationic nature of netropsin. In the case of netropsin binding to *Pseudoknot*, the observed thermodynamic differences may be due to the lower length of the loop at the 5′ end of A_3T_2 yielding the A_3T_2 site with a more exposed minor groove or less helical in nature. This can be accounted by the difference in the type and quantity of the water released by *Pseudoknot*, which correlates with the observed entropy differences. For instance, the lower release of 8 water molecules by *Pseudoknot* may be contributing with an endothermic enthalpy of ~2.4 kcal/mol^{-1}. It takes 300 cal/mol^{-1} to remove 1 mol of water from DNA [63]. This term may well account for the lower ΔH_bs of netropsin binding to *Hairpin* and *Hammer*.

Table 3
Thermodynamic profiles for the interaction of netropsin with hairpins.

$K_b \times 10^{-7}$ (M^{-1})	ΔG°_b (kcal/mol)	ΔH_b (kcal/mol)	$T\Delta S_b$ (kcal/mol)	ΔV (cm^3/mol)	$\Delta\Phi K_S \times 10^4$ (cm^3/mol bar)
Hairpin					
2.4	−9.5	−8.9	0.6	38.8	102.3
Hammer					
3.2	−9.7	−7.6	2.1	37.5	98.5
(0.2)	(−8.1)	(−21.5)	(−13.4)		
Pseudoknot					
0.1	−7.4	−12.2	−4.8	30.8	44.8

Standard thermodynamic profiles were determined in 10 mM sodium phosphate buffer, 0.1 M NaCl at pH 7 and 10 °C, whereas the hydration parameters of the 1:1 complexes were determined in 10 mM Hepes, 100 mM NaCl, at pH 7.5 and15 °C, and calculated per mole of netropsin. The experimental uncertainties are as follows: ΔH_b and ΔG_b° (±5%), $T\Delta S$ (±8%). ΔV (±7%), ΔK_S (±2.5×10^4).

3.5. Interaction of random copolymers with hairpins

In the previous sections, we have shown that all three DNA hairpins formed their respective secondary structures and the minor groove ligand netropsin associates to the A_3T_2 site, located at their end stems, with tight affinity and specificity. Furthermore, we also showed that the incorporation of the loops renders these stem-loop motifs slightly more hydrophobic, making them perhaps suitable to cross lipid membranes of the cell. In addition, these intramolecular DNA complexes have long sequences that can be used to mimic the secondary structures presented by RNA molecules, and in the control of gene expression using antigene and antisense strategies. For the stated reasons, this section presents the interaction of hairpins with random copolymers, using an ethidium displacement essay. We are testing the hypothesis that formation of hairpin–copolymer complexes with moderate affinities should help the cellular delivery of hairpins. In addition, the copolymer should protect the DNA hairpin against the action of nucleases. Fig. S4 shows a typical experiment, the fluorescence spectrum of a saturated ethidium–hairpin complex is the top spectrum, addition of copolymer displaces bound ethidium, resulting in the lowering of its fluorescence intensity at 600 nm. The concentration of copolymer that displaces 50% of the bound ethidium is used to calculate the copolymer binding affinity. Table 4 lists all the binding affinities, K_{COP}, for the binding of three copolymers with 38% (P_{38}), 51% (P_{51}) and 68% (P_{68}) of polyethylene glycol segments. These K_{COP}s range from 7.4×10^4 M^{-1} (*Hairpin*—P_{68}) to 2.3×10^6 M^{-1} (*Pseudoknot*—P_{38}). For a given copolymer, the K_{COP} increases tenfold from *Hairpin* to *Hammer* to *Pseudoknot*, indicating that the interaction of the copolymer is more favorable with the more hydrophobic hairpin, the *Pseudoknot*. For a given hairpin, K_{COP}s decreases slightly, by an average factor of 3, with the increase in the percentage of PEG of the copolymer; however, with *Pseudoknot* the decrease is the lowest (factor of 5). The overall results show that we do get suitable copolymer binding affinities with the more hydrophobic hairpin, confirming our hypothesis that these types of complexes can be used in the cellular delivery of oligonucleotides to control the expression of genes.

4. Conclusion

We used a combination of biophysical techniques to determine complete thermodynamic profiles, including hydration, for the unfolding of DNA intramolecular stem-loop motifs and their interaction with both the minor groove ligand netropsin and random cationic copolymers. All hairpins adopted the B-like conformation. All transitions in these hairpins take place according to their melting domains, and their thermodynamic profiles are consistent with existing DNA nearest-neighbors parameters. Overall, this information will improve our current picture of how sequence and loops control the stability and melting behavior of nucleic acids, supplementing

Table 4
K_{COP}s (M^{-1}) for the interaction of copolymers with hairpins.

P_{38}	P_{51}	P_{68}
Hairpin		
2.4×10^5	1.9×10^5	7.4×10^4
Hammer		
1.4×10^6	9.7×10^5	4.9×10^5
Pseudoknot		
2.3×10^6	1.6×10^6	1.1×10^6

All K_{COP}s determined in 10 mM sodium phosphate buffer, 0.1 M NaCl at pH 7 and 15 °C. The experimental error in their determination is 50%.

current nearest-neighbor parameters in predicting secondary structure from knowledge of the sequence. Furthermore, absolute hydration parameters showed that all hairpins are well hydrated; the inclusion of loop(s) shifted their hydrophilic–hydrophobic equilibria towards slightly more hydrophobic i.e., loops immobilize structural water. This is shown in their interaction with cationic copolymers, the more hydrophobic hairpin (*Pseudoknot*) binds better ($K_b = 10^6\ M^{-1}$).

Binding of netropsin to the A_3T_2 site of each hairpin takes place with tight affinities (~$10^7\ M^{-1}$), the exception is *Pseudoknot* (~$10^6\ M^{-1}$), high exothermic enthalpies (−7.6 to −12.2 kcal/mol^{-1}), and 1:1 stoichiometries. However, the one exception is the secondary site in *Hammer* that showed an unusual exothermicity of −22 kcal/mol, most likely from the formation of additional base-pair stacks at the junction site. Netropsin binding releases electrostricted water (*Hairpin* and *Hammer*) and structural water (*Pseudoknot*).

Finally, the overall data should help in the optimization of oligonucleotide reagents for the targeting of specific transient structures that form *in vivo*.

Acknowledgement

This work was supported by Grants MCB-0315746 and MCB-0616005 from the National Science Foundation, and a Shared Instrumentation Grant 1S10RR027205 from the National Institutes of Health. We thank Professor Edward Roche for the editorial help. The assistance of Professor Jurij Lah (from the University of Ljubljana, Slovenia) with the global fitting of the *Net-Hairpin* binding isotherm is greatly appreciated.

Appendix A. Supplementary data

Supplementary data to this article can be found online at doi:10.1016/j.bpc.2011.06.006.

References

[1] P.F. Johnson, S.L. McKnight, Eukaryotic transcriptional regulatory proteins, Annu. Rev. Biochem. 58 (1989) 799–839.
[2] N. Panayotatos, R.D. Wells, Cruciform structures in supercoiled DNA, Nature 289 (1981) 466–470.
[3] D.M.J. Lilley, The inverted repeat as a recognizable structural feature in supercoiled DNA molecules, Proc. Natl. Acad. Sci. U. S. A. 77 (1980) 6468–6472.
[4] Y. Pollack, R. Stein, A. Razin, H. Cedar, Methylation of foreign DNA sequences in eukaryotic cells, Proc. Natl. Acad. Sci. U. S. A. 77 (1980) 6463–6467.
[5] D.M.J. Lilley, Hairpin-loop formation by inverted repeats in supercoiled DNA is a local and transmissible property, Nucleic Acids Res. 9 (1981) 1271–1290.
[6] K.J. Breslauer, R. Frank, H. Blocker, L.A. Marky, Predicting DNA duplex stability from the base sequence, Proc. Natl. Acad. Sci. U. S. A. 83 (1986) 3746–3750.
[7] T. Xia, J. SantaLucia Jr., M.E. Burkard, R. Kierzek, S.J. Schroeder, X. Jiao, C. Cox, D.H. Turner, Thermodynamic parameters for an expanded nearest-neighbor model for formation of RNA duplexes with Watson–Crick base pairs, Biochemistry 37 (1998) 14719–14735.
[8] J. SantaLucia Jr., H.T. Allawi, P.A. Seneviratne, Improved nearest-neighbor parameters for predicting DNA duplex stability, Biochemistry 35 (1996) 3555–3562.
[9] N. Sugimoto, S. Nakano, M. Katoh, A. Matsumura, H. Nakamuta, T. Ohmichi, M. Yoneyama, M. Sasaki, Thermodynamics parameters to predict stability of RNA/DNA hybrid duplexes, Biochemistry 34 (1995) 11211–11216.
[10] D. Rentzeperis, R. Shikiya, S. Maiti, J. Ho, L.A. Marky, Folding of intramolecular DNA hairpin loops: enthalpy–entropy compensations and hydration contributions, J. Phys. Chem. B 106 (2002) 9945–9950.
[11] L.A. Marky, S. Maiti, C. Olsen, R. Shikiya, S. Johnson, M. Kaushik, I. Khutsishvilli, in: V. Labhasetwar, D.L. Leslie-Pelecky (Eds.), Building blocks of nucleic acid nanostructures: unfolding thermodynamics of intramolecular DNA complexes, Biomedical Applications of Nanotechnology, John Wiley and Sons, Inc., 2007, pp. 191–226.
[12] H.-T. Lee, C.M. Olsen, L. Waters, H. Sukup, L.A. Marky, Thermodynamic contributions of the reactions of DNA intramolecular structures with their complementary strands, Biochimie 90 (2008) 1052–1063.
[13] H.-T. Lee, C. Carr, H. Siebler, L. Waters, I. Khutsishvili, F. Iseka, B. Domack, C.M. Olsen, L.A. Marky, A thermodynamic approach for the targeting of nucleic acid structures using their complementary single strands, Methods Enzymol. 492 (2011) 1–26.
[14] L.A. Marky, K.J. Breslauer, The origins of netropsin binding affinity and specificity: correlation of thermodynamic and structural data, Proc. Natl. Acad. Sci. U. S. A. 84 (1987) 4359–4363.
[15] D. Rentzeperis, T.J. Dwyer, B.H. Geierstanger, J.G. Pelton, D.E. Wemmer, L.A. Marky, Interaction of minor groove ligands to an AAATT/AATTT site: correlation of thermodynamic characterization and solution structure, Biochemistry 34 (1995) 2937.
[16] W. Saenger, Principles of nucleic acid structure, Springer-Verlag, New York, 1984.
[17] J. Texter, Nucleic acid–water interactions, Prog. Biophys. Mol. Biol. 33 (1978) 83.
[18] E. Westhof, Water: an integral part of nucleic acid structure, Annu. Rev. Biophys. Biophys. Chem. 17 (1988) 125–144.
[19] H.M. Berman, Hydration of DNA, Curr. Opin. Struct. Biol. 1 (1991) 423.
[20] M.J. Tunis, J.E. Hearst, Hydration of DNA. II. Base composition dependence of the net hydration of DNA, Biopolymers 6 (1968) 1345–1353.
[21] D. Rentzeperis, D.W. Kupke, L.A. Marky, Volume changes correlate with entropies and enthalpies in the formation of nucleic acid homoduplexes: differential hydration of A and B conformations, Biopolymers 33 (1993) 117–125.
[22] G.M. Mrevlishvili, Dependence of hydration on GC content of natural DNA, Dokl. Akad. Nauk SSSR 260 (1981) 761–764.
[23] V.A. Buckin, B.I. Kankiya, N.V. Bulichov, A.V. Lebedev, V.P. Gukovsky, A.P. Sarvazyan, A.R. Williams, Measurement of anomalously high hydration of (dA)n·(dT)n double helixes in dilute solution, Nature 340 (1989) 321–322.
[24] R.B. Macgregor Jr., M.Y. Chen, Delta V0 of the Na(+)-induced B–Z transition of poly[d(G–C)] is positive, Biopolymers 29 (1990) 1069–1076.
[25] V.A. Buckin, B.I. Kankiya, A.P. Sarvazyan, H. Uedaira, Acoustical investigation of poly(dA).poly(dT), poly[d(A–T)], poly(A).poly(U) and DNA hydration in dilute aqueous solutions, Nucleic Acids Res. 17 (1989) 4189–4203.
[26] T. Umehara, S. Kuwabara, S. Mashimo, S. Yagihara, Dielectric study on hydration of B-, A-, and Z-DNA, Biopolymers 30 (1990) 649–956.
[27] R.S. Preisler, H.H. Chen, M.F. Colombo, Y. Choe, B.J. Short Jr., D.C. Rau, The B form to Z form transition of poly(dG-m5dC) is sensitive to neutral solutes through an osmotic stress, Biochemistry 34 (1995) 14400–14407.
[28] D. Rentzeperis, D.W. Kupke, L.A. Marky, Differential hydration of dA·dT base pairs in parallel-stranded DNA relative to antiparallel DNA, Biochemistry 33 (1994) 9588–9591.
[29] H.S. Frank, M.W. Evans, Free volume and entropy in condensed systems. III. Entropy in binary liquid mixtures; partial molal entropy in dilute solutions; structure and thermodynamics in aqueous electrolytes, J. Chem. Phys. 13 (1945) 507–532.
[30] W. Kauzmann, in: C.B. Anfinsen Jr. (Ed.), Some factors in the interpretation of protein denaturation, Advances in Protein Chemistry, vol. 14, Academic Press Inc., New York, 1959, p. 1.
[31] F.J. Millero, in: R.A. Horn (Ed.), Structure and transport processes, Water and Aqueous Solutions, John Wiley & Sons, New York, 1972, p. 519.
[32] V.A. Buckin, B.I. Kankiya, D. Rentzeperis, L.A. Marky, Mg^{2+} recognizes the sequence of DNA through 1st hydration shell, J. Am. Chem. Soc. 116 (1994) 9423–9429.
[33] V.A. Buckin, H. Tran, V. Morozov, L.A. Marky, Hydration effects accompanying the substitution of counterions in the ionic atmosphere of poly(rA)·2poly(rU) helices, J. Am. Chem. Soc. 118 (1996) 7033–7039.
[34] C.R. Cantor, M.M. Warshaw, H. Shapiro, Oligonucleotide interactions. III. Circular dichroism studies of the conformation of deoxyoligonucleotides, Biopolymers 9 (1970) 1059–1077.
[35] L.A. Marky, K.S. Blumenfeld, S. Kozlowski, K.J. Breslauer, Salt-dependent conformational transitions in the self-complementary deoxydodecanucleotide d(CGCGAATTCGCG): evidence for hairpin formation, Biopolymers 22 (1983) 1247–1257.
[36] C.K. Nisha, S.V. Manorama, M. Ganguli, S. Maiti, J.N. Kizhakkedadathu, Complexes of Poly(ethylene glycol)-based cationic random copolymer and calf thymus DNA: a complete biophysical characterization, Langmuir 19 (2004) 2386–2396.
[37] L.A. Marky, K.J. Breslauer, Calculating thermodynamic data for transitions of any molecularity from equilibrium melting curves, Biopolymers 26 (1987) 1601–1620.
[38] D. Rentzeperis, J. Ho, L.A. Marky, Contribution of loops and nicks to the formation of dumbbells: melting behavior and ligand binding, Biochemistry 32 (1993) 2564–2572.
[39] D. Rentzeperis, L.A. Marky, Netropsin binding as a thermodynamic probe of the grooves of parallel DNA, J. Am. Chem. Soc. 115 (1993) 1645–1650.
[40] G.S. Manning, Molecular theory of polyelectrolyte solution with application to electrostatic properties of polynucleotides, Q. Rev. Biophys. 11 (1978) 179–246.
[41] C.R. Cantor, P.R. Schimmel, Biophysical Chemistry, W.H. Freeman and Company, New York, 1980.
[42] M. Kaushik, N. Suehl, L.A. Marky, Calorimetric unfolding of the bimolecular and i-motif complexes of the human telomere complementary strand, $d(C_3TA_2)_4$, Biophys. Chem. 126 (2007) 154–164.
[43] T. Wiseman, S. Williston, J.F. Brandts, L.-N. Lin, Rapid measurement of binding constants and heats of binding using a new titration calorimeter, Anal. Biochem. 179 (1989) 131–137.
[44] B. Pagano, C.A. Mattia, C. Giancola, Applications of isothermal titration calorimetry in biophysical studies of G-quadruplexes, Int. J. Mol. Sci. 10 (2009) 2935–2957.
[45] J. Lah, I. Drobnak, M. Dolinar, G. Vesnaver, What drives the binding of minor groove-directed ligands to DNA hairpins? Nucleic Acids Res. 36 (2008) 897–904.
[46] F. Eggers, T. Funck, Ultrasonic measurements with milliliter liquid samples in the 0.5-100 MHz range, Rev. Sci. Instrum. 44 (1973) 969–977.
[47] S. Barnartt, The velocity of sound in electrolytic solutions, J. Chem. Phys. 20 (1952) 278–279.
[48] H. Shio, T. Ogawa, H. Yoshihashi, Measurement of the amount of bound water by untrasonic inferometer, J. Am. Chem. Soc. 77 (1955) 4980–4982.

[49] A.R. Morgan, J.S. Lee, D.F. Pulleyblank, N.L. Murray, D.H. Evans, Ethidium fluorescence assays. Part 1. Physicochemical studies, Nucleic Acids Res. 7 (1979) 547–569.
[50] D. Rentzeperis, Thermodynamics and ligand interactions of DNA hairpins. Doctoral Dissertation (New York University, New York, NY, 1995) p. 246.
[51] S.B. Howerton, C.C. Sines, D. VanDerveer, L.D. Williams, Locating monovalent cations in the grooves of B-DNA, Biochemistry 40 (2001) 10023–10031.
[52] B. Kankia, L.A. Marky, DNA, RNA and DNA/RNA Oligomer Duplexes: A Comparative Study of Their Stability, Heat, Hydration and Mg^{2+} Binding Properties, J. Phys. Chem. B 103 (1999) 8759–8767.
[53] B.I. Kankia, V. Buckin, V.A. Bloomfield, Hexamminecobalt(III)-induced condensation of calf thymus DNA. Circular dichroism, ultrasonic and density measurements, Nucleic Acids Res. 29 (2001) 2795–2801.
[54] F.J. Millero, G.K. Ward, F.K. Lepple, E.V. Hoff, Isothermal compressibility of aqueous sodium chloride, magnesium chloride, sodium sulfate, and magnesium sulfate solutions from 0 to 45.deg. at 1 atm, J. Phys. Chem. 78 (1974) 1636–1643.
[55] A. Lo Surdo, F.J. Millero, Apparent molal volumes and adiabatic compressibilities of aqueous transition metal chlorides at 25 °C, J. Phys. Chem. 84 (1980) 710–715.
[56] B.I. Kankia, T. Funck, H. Uedaira, V.A. Buckin, Volume and compressibility effects in the formation of meEDTA complexes, J. Sol. Chem. 26 (1997) 877–890.
[57] V.A. Buckin, B.I. Kankiya, N.V. Bulichov, A.V. Lebedev, I.Ya. Gukovsky, V.P. Chuprina, A.P. Sarvazyan, A.R. Williams, Measurement of anomalously high hydration of $(dA)_n \cdot (dT)_n$ double helices in dilute solution, Nature 340 (1989) 321–322.
[58] V.A. Buckin, Hydration of nucleic bases in dilute aqueous solutions. Apparent molar adiabatic and isothermal compressibilities, apparent molar volumes and their temperature slopes at 25 °C, Biophys. Chem. 29 (1988) 283–292.
[59] L.A. Marky, D.W. Kupke, Probing the hydration of the minor groove of A·T synthetic DNA polymers by volume and heat changes, Biochemistry 28 (1989) 9982–9988.
[60] L.A. Marky, D.W. Kupke, Enthalpy–entropy compensation in nucleic acids: contribution of electrostriction and structural hydration, Methods Enzymol. 323 (2000) 419–441.
[61] T.V. Chalikian, G.E. Plum, A.P. Sarvazyan, K.J. Breslauer, Influence of drug binding on DNA hydration: acoustic and densimetric characterizations of netropsin binding to the poly(dAdT).poly(dAdT) and poly(dA).poly(dT) duplexes and the poly(dT).poly(dA). poly(dT) triplex at 25 degrees C, Biochemistry 33 (1994) 8629–8640.
[62] C.M. Olsen, W.H. Gmeiner, L.A. Marky, Unfolding of G-quadruplexes: energetic, and ion and water contributions of G-quartet stacking, J. Phys. Chem. B 110 (2006) 6962–6969.
[63] A.I. Gasan, V.Y. Maleev, M.A. Semenov, Role of water in stabilizing the helical biomacromolecules DNA and collagen, Stud. Biophys. 136 (1990) 171–178.